

## Abrupt Seasonal Changes of Surface Climate Observed in Northern Mongolia by an Automatic Weather Station

By Shin Miyazaki, Tetsuzo Yasunari

*Institute of Geoscience, University of Tsukuba, Tsukuba, Japan*

and

Tsohiogiin Adyasuren

*Ministry of Nature and Environment, Mongolia*

*(Manuscript received 7 May 1998, in revised form 27 January 1999)*

### Abstract

Continuous observations of surface meteorological elements have been carried out since September 30, 1993, to study the roles of land surface processes in seasonal climate variation. The observations were taken by the AANDERA Automatic Weather Station (AWS) at Baruunkharaa (48°55'N, 106°4'E) in northern Mongolia. This location is the center of the source region of the Siberian high, which is a major center of action for the winter climate and atmospheric circulation over the Eurasian Continent.

Abrupt changes of air temperature and specific humidity were detected during the course of seasonal change from October 1993 to September 1994. The annual cycle was divided into four seasons, based on the timing of these abrupt changes: *i.e.*, winter (mid-November to early March), spring (mid-March to early June), summer (mid-June to later August) and autumn (early September to early November). Over several days in mid-November the air temperature decreased about 20°C, concurrent with an increase in the albedo from 0.5 to 0.9. A coreless winter was characterized by a near constant air temperature of about -15°C or less, along with a high albedo of more than 0.5: *i.e.*, continuous snow cover except for the period from mid-February to early March. Winter ended with a sudden increase of air temperature of about 20°C during several days in mid-March. Spring was characterized by the development of the daytime mixed layer, as suggested from the afternoon decrease of specific humidity. An abrupt increase of specific humidity of about 5 gkg<sup>-1</sup> — which occurred in mid-June — coincided with the onset of the summer season. During summer, the daytime increase of specific humidity attained its annual maximum, this is likely due to strong evaporation from the surface. In early September, the specific humidity dropped by about 5 gkg<sup>-1</sup> over a period of several days. The characteristics of the autumn onset were nearly the same as spring, except for the absence of afternoon decrease in specific humidity, which implied that the diurnal growth of the mixed layer was not strong enough to create a strong entrainment.

### 1. Introduction

The East Asia winter climate is strongly controlled by the state and variability of both the Siberian high and Aleutian low. Mongolia, located in the interior of the Eurasian continent coincides with the core of the action center, *i.e.*, the Siberian high. During summer, the monsoon trough — a

heat low of the Asian summer monsoon — extends to Mongolia. Therefore, this area exhibits the greatest difference in monthly mean sea level pressure between summer and winter found over Earth's surface. Ding and Krishnamurti (1987) suggested that strong radiative cooling, and large scale descending motions over this region, contribute to the rapid buildup of the Siberian high.

In the early summer, structural changes in the Baiu front in China, and the northward shift of the polar front in Eurasia, are likely to occur as a response to the seasonal surface heating in the semi-arid region from Takla Makan, North China, and the

Corresponding author: Shin Miyazaki, Institute of Geoscience, University of Tsukuba, 1-1-1 Tennoudai, Tsukuba 305-8571, Japan. E-mail: shin@erc2.suiri.tsukuba.ac.jp

©1999, Meteorological Society of Japan

## Location Map

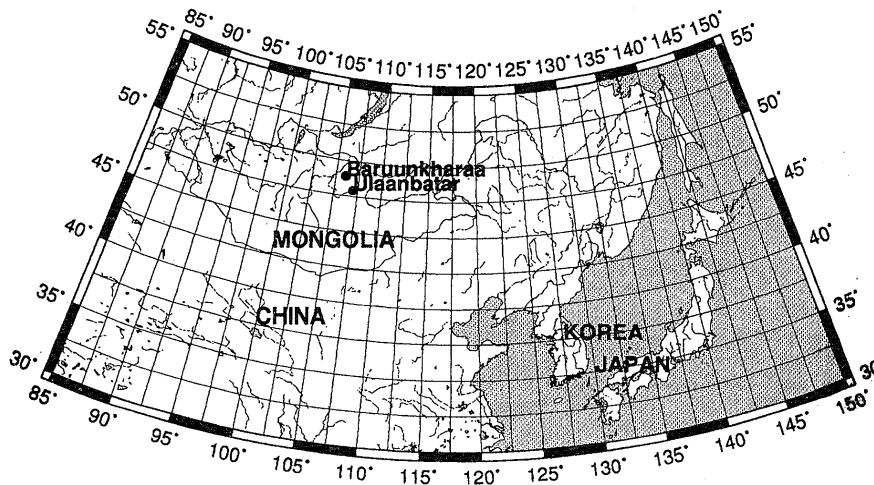


Fig. 1. Map showing the location of the observation site.

Mongolian Plateau (Kato, 1985, 1987; among others.) Details of the seasonal heating process in the interior of the Eurasian Continent, however, have not yet been clarified.

This area, as part of northern Eurasia, has been undergoing rapid warming during the past several decades (IPCC, 1992, 1995). Groisman *et al.* (1994) suggested that the systematic retreat of snow cover extent during the past 20 years was related to a change in the snow cover feedback, affecting the radiative balance and leading to increased spring-time temperatures. It was also pointed out that the inadequacy of the thermometric data used in their analyses, together with a highly variable snow cover extent over western China, Mongolia, and the Himalayas, indicated that a more thorough analysis with more comprehensive data in these regions was required. Yatagai and Yasunari (1994) pointed out that the linear trend of increasing annual mean temperature was remarkable during the recent 40 year period (1951–1990), especially in the northern regions of China and Mongolia. This increasing trend in the annual mean temperature is mainly due to warmer winter and spring temperature. The causes and/or physical processes that produce this warming trend in the region have not been clarified.

To solve these problems, more information is required concerning the physical processes of the diurnal and seasonal variations of surface climate conditions, and the associated surface radiation and heat balance over Mongolia. The purpose of this study is to investigate the characteristics of the seasonal and diurnal changes of surface climate and associated land surface processes over Mongolia. Surface meteorological elements gathered by an automatic weather station (AWS) have been continuously ob-

served since September 30, 1993, at Baruunkharaa (48°55'N, 106°4'E) in the northern region of Mongolia. We will describe the characteristics of the diurnal and seasonal variations of surface climate, with some discussion also focussed on the role that land surface conditions play in the seasonal cycle.

### 2. Observation of surface meteorological elements

#### 2.1 The observational site

For the purposes of this study, the Baruunkharaa observational site (48°55'N, 106°4'E) was chosen, located in a wide valley on the Mongolian Plateau, about 150 km north of Ulan Bator, the capital of Mongolia (Fig. 1). The observational site is located near the center of the village of Baruunkharaa, which has a population of about 4000, and covering an area of 11,000 km<sup>2</sup>. The elevation of the site is 806.9 m above sea level. Baruunkharaa has a semi-arid climate, covered by grass in the summer. During the winter, the site closely corresponds to the Siberian high center. The long-term annual mean air temperature and annual precipitation for Baruunkharaa are -1.4°C and 265.1 mm, respectively.

To clarify the climatic characteristics of the observational site, Fig. 2 shows climatological January and July mean sea level pressure (SLP) maps over and around Mongolia produced from the Global Historical Climatology Network (GHCN) data consisting of about 40 years (1951–1988), and 18 stations in Mongolia during 30 years (1961–1990). Large differences in the SLP are obviously found between January and July. During January, the center core of the Siberia-Mongolia high exceeding 1040 hPa, is located over northern Mongolia. Differences in SLP were very small over Mongolia in July. The Hentei

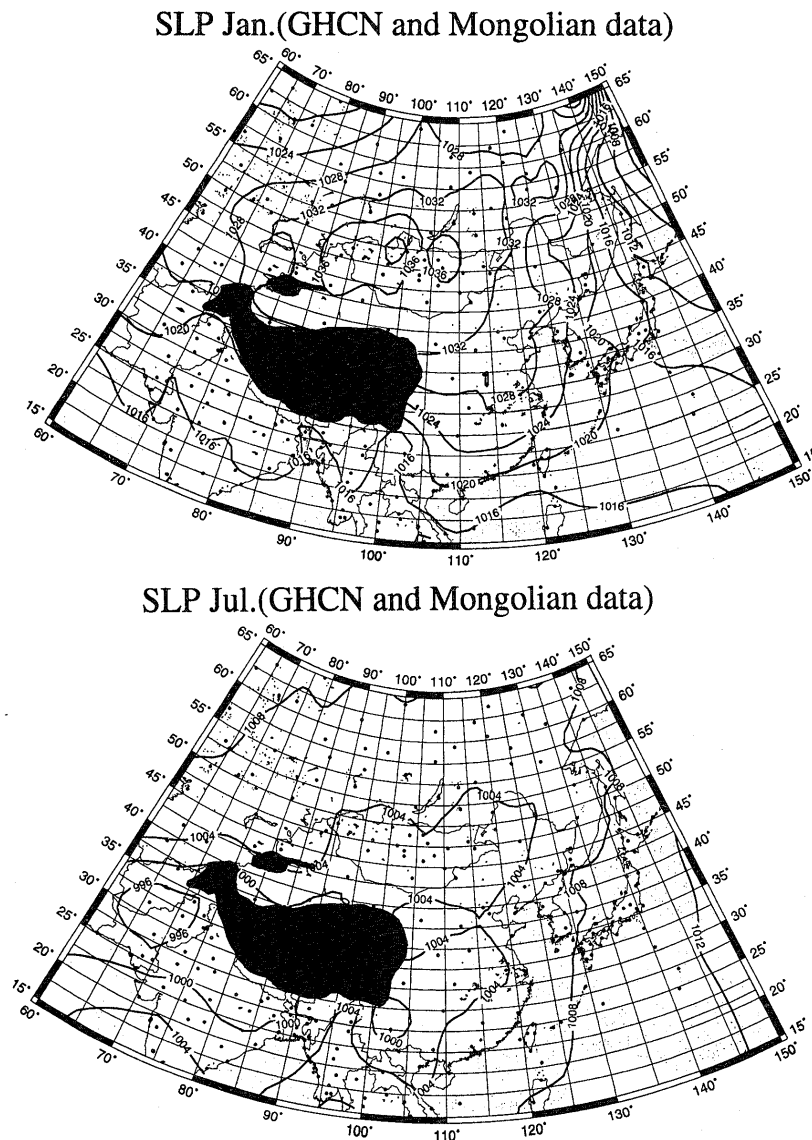


Fig. 2. Climatological monthly mean sea level pressure maps over and around Mongolia from data at about 140 GHCN stations and 18 Mongolian stations for January (a) and July (b). Solid circles indicate the location of the stations. Darkened area indicates regions with mean elevations of 3000 m or higher above sea level.

Mountain range with elevations of 1800~2800 m, being one of the highest regions of the Mongolian Plateau, is located about 180 km southeast of the site. The Burengiun Mountain range — with elevations of 1500~2000 m — is located about 150 km to the northwest of the site. The Hara River runs from south to north, about 500 m east of the site. The width of the valley is about 50 km, and no big mountains are located within a radius of 100 km of the site.

2.2 Method of surface meteorological element observation

The AWS (AANDERA 2704) has been used for long-term monitoring of surface meteorological elements from September 1993 to September 1998. The

AWS consists of a 3-cup anemometer for measuring wind speed, a resistance thermometer for temperature, a hygroscopic humidity meter for relative humidity, and two pyranometers to measure downward and upward solar radiation. The air temperature, relative humidity, and wind speed are measured at heights of 1 m and 4 m, while the downward and upward solar radiation are observed at 4 m above the ground surface. The sensors of the thermometers and humidity meters are covered with radiation shields, made from nylon with diameters of about 60 mm. The nylon allows for natural ventilation through the radiation shields. Soil surface temperatures  $T_s$  are measured by a platinum-resistance thermometer, set on the ground surface and covered with

Table 1. The elements, sensors, accuracy and frequency of the AWS.

Elements	Sensors	Accuracy	Manufacturer	Frequency
Air temperature	Platinum Resister	$\pm 0.1^\circ\text{C}$	Aandera Co. (No. 3145)	Every 30 min. Instantaneous value
Wind speed	3-cup type	0.2 % or 0.2 m/s whichever greater	same (No. 2740)	30 min. mean or 30 min. max
Relative humidity	Hygroscopic hair	$\pm 3\%$ RH	same (No. 2820)	Every 30 min. Instantaneous value
Global solar rad.	Pyranometer Temperature difference type (0.3–2.5 $\mu\text{m}$ )	Better than $\pm 20\text{ W/m}^2$	same (No. 2770)	same
Soil surface temperature	Platinum Resistor	$\pm 0.1^\circ\text{C}$	same (No. 3145)	same

a thin layer of soil. During the summer, the Ts thermometer is placed under short grass which reached a height of about 30 cm, while in the winter, under a thin snow cover which accumulated to as much as several cm. The system is operated by a solar cell power module, with data recorded every 30 minutes since October, 1993. The wind speed measurements are taken as 30-minute averages, while other surface meteorological elements are measured as an instantaneous value. The elements, sensors, accuracy, and frequency of the AWS system are listed in Table 1.

Potential temperature and specific humidity were calculated from the air temperature and relative humidity of the AWS data and air pressure from the Baruunkharaa Station data. Precipitation, air pressure, and soil temperature from the Baruunkharaa station, and climatological monthly-mean sea level pressure at 18 stations in Mongolia were provided by the Ministry of Nature and Environment of Mongolia.

### 3. Seasonal and diurnal changes of surface meteorological elements

#### 3.1 Seasonal change

Figure 3 shows the time series of daily mean values of air temperature, specific humidity, albedo, and daily precipitation from October 1993 to September 1994. During several days in mid-November the air temperature exhibited a sudden decrease of about 20 degrees to  $-20^\circ\text{C}$ , while the albedo simultaneously increased from 0.5 to 0.9. During the period from mid-November to mid-February, the albedo exceeded 0.5 and the air temperature remained fairly level less than  $-15^\circ\text{C}$ . Such a variation of air temperature is called a “coreless winter,” which is typical of polar regions, particularly in Antarctica. Van Loon (1967) discussed this phenomenon for the Antarctica winter (July to September), which is sup-

posed to result from interactions between the intensity of seasonally varying advection from the surrounding sea and radiation cooling over the continent. It is not clear, however, if the cause of the coreless winter in Mongolia is the same as that formed in Antarctica. A further study with a large-scale circulation will be necessary, although it can be speculated that the coreless winter occurred due to both the decreased radiative cooling to nearly zero, and the weakening of warm air advection from the coastal area. Although the albedo decreased to less than 0.4 in mid-February, both the air temperature and Ts remained low until mid-March. Spiky increases of albedo can be seen in early March and early April, which may imply snowfall, but the snow cover did not become continuous. The air temperature suddenly increased by about 20 degrees to near  $0^\circ\text{C}$  in mid-March, and gradually increased afterwards through the seasonal march until mid-June. In mid-June, an abrupt increase of specific humidity occurred, and remained at a near constant value of  $10\text{ gkg}^{-1}$  or more, with the air temperature maintained a level of about  $20^\circ\text{C}$  until the end of August. This period can be defined as summer. The abrupt increase of specific humidity occurred after heavy precipitation. In Baruunkharaa, most of the precipitation (about 70 % of the annual precipitation) occurs during the summer season, from June to August. The reason for the sudden increase in specific humidity can be speculated as due to a rapid increase in evapotranspiration from the surface. That is, surface soil moisture and surface vegetation increased due to the large amount of precipitation. Kato *et al.* (1995) pointed out that many deep convective clouds, with horizontal scales less than 100 km in diameter, existed around 40–50°N/105–125°E at 12 UTC on 13 July 1979. The period of their analysis, however, does not exactly

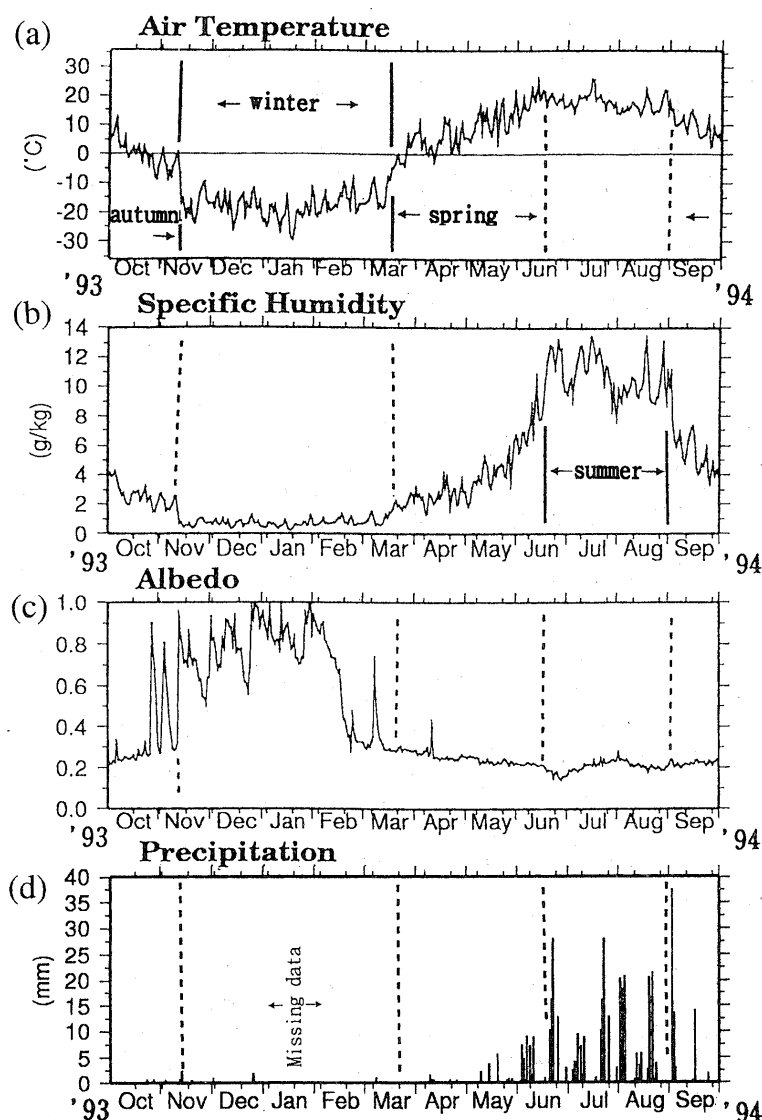


Fig. 3. Time series of daily mean values of air temperature (a), specific humidity (b), albedo (c), and precipitation (d) from October 1993 to September 1994 as observed at Baruunkharaa.

coincide with that in the present study, and further analysis with large scale cloud distribution should be attempted. The specific humidity exhibited a sharp decrease of  $5 \text{ gkg}^{-1}$  in early September, while the air temperature began to gradually decrease with time toward the next winter.

As shown in Fig. 3, a number of abrupt changes can be found in the air temperature and specific humidity of the AWS data during the period from October 1993 to September 1994. The annual cycle can be sub divided into four seasons based on the timing of these abrupt changes: namely, winter (mid-November to early March), spring (mid-March to early June), summer (mid-June to late August), and autumn (early September to early November).

Figure 4 shows the time series of the daily maximum and minimum values of air temperature, specific humidity, wind speed, and the daily accumu-

lated values of downward and upward solar radiation from October 1993 to September 1994. The diurnal range of air temperature was about  $20^\circ\text{C}$  over the entire year except for summer (mid-June to late August), when it decreased to about  $10^\circ\text{C}$ . In contrast, the diurnal range of specific humidity was large from mid-June to late August (about  $5 \text{ gkg}^{-1}$ ), but smaller in winter (from mid-November to early March). It is likely that evaporation from the surface suppressed any increase of the air temperature and maintained a near constant high value of specific humidity during the summer. The annual mean value of the diurnal range of wind speeds was about  $3 \text{ ms}^{-1}$ , and exhibited an annual minimum of about  $2 \text{ ms}^{-1}$  or less in the winter. During the spring season, the diurnal range of the wind speed displayed an annual maximum exceeding  $4 \text{ ms}^{-1}$ , and the number of days that the daily maximum wind speed ex-

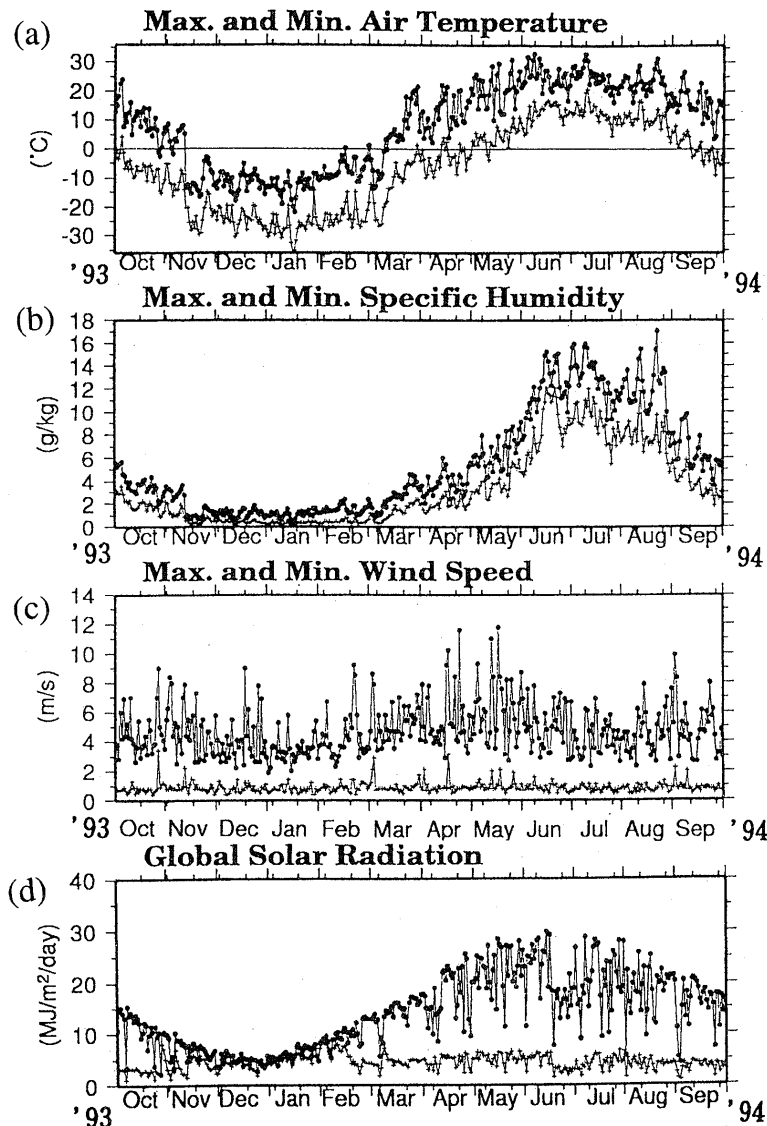


Fig. 4. Time series of daily maximum and minimum values of air temperature (a), specific humidity (b), mean wind speed (c), and daily accumulated global downward and upward solar radiation (d) from October 1993 to September 1994 as observed at Baruunkharaa.

ceeded  $8 \text{ ms}^{-1}$  was greater than 10 days, whereas 5 days or less in the other seasons. The diurnal range of the wind speed was about  $3 \text{ ms}^{-1}$  in the summer. Although the annual mean maximum wind speed was about  $3 \text{ ms}^{-1}$ , only the months of April and May displayed mean maximum wind speeds in excess of  $5 \text{ ms}^{-1}$ . Strong winds with dust storms or snowstorms occasionally occurred in spring, which resulted in serious damage to livestock. The diurnal change of wind speed will be further discussed in Subsection 3.2. From mid-April to early June, downward solar radiation displayed an annual maximum of approximately  $25 \text{ MJm}^{-2}\text{day}^{-1}$ . In early June, the downward solar radiation suddenly decreased by  $10 \text{ MJm}^{-2}\text{day}^{-1}$ , due to an increase of cloudiness and rainy conditions that occurred during the summer. The difference between the downward

and upward solar radiation was very small from the middle of November to mid-February with a value of  $5 \text{ MJm}^{-2}\text{day}^{-1}$  or less, corresponding to the high albedo of the snow cover. The difference was greater than  $10 \text{ MJm}^{-2}\text{day}^{-1}$  during the course of the other seasons.

Time series of the daily mean, daily maximum, and daily minimum  $T_s$ , and the diurnal range of  $T_s$  from October 1993 to September 1994 are shown in Fig. 5. The seasonal variation of daily mean  $T_s$  exhibited nearly the same features as the air temperature. When the daily maximum  $T_s$  reached its maximum in May (about  $50^\circ\text{C}$ ), the downward solar radiation also reached its annual maximum. The diurnal range of  $T_s$  was small, being about 10 degrees from mid-November to mid-February. The diurnal range of  $T_s$  was also small during the summer and Septem-

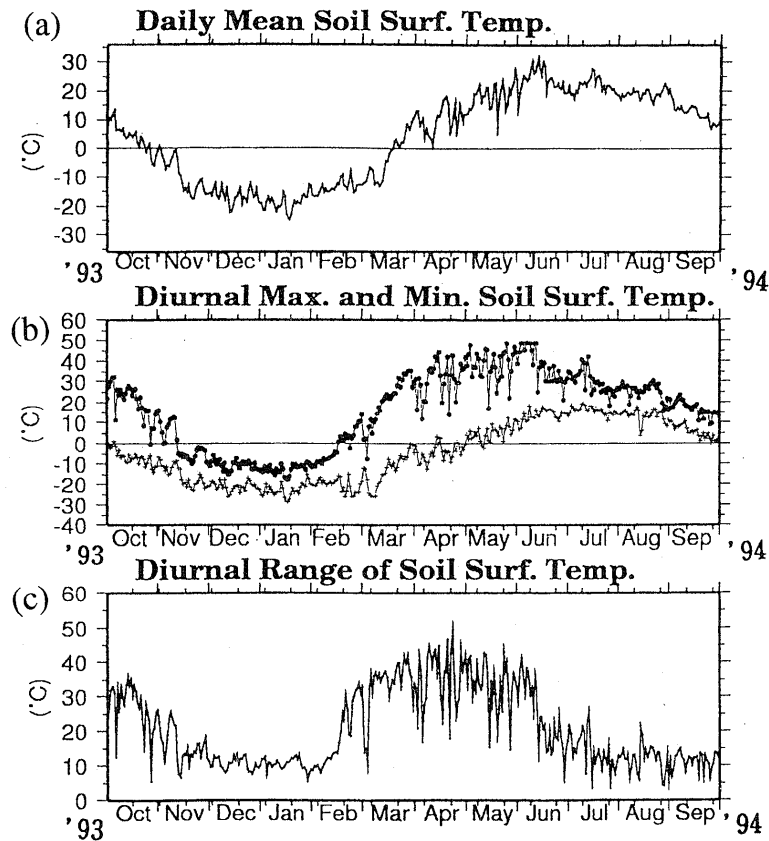


Fig. 5. Time series of daily mean (a), daily maximum, minimum (b), and diurnal range of Ts (c) from October 1993 to September 1994 as observed at Baruunkharaa.

ber, corresponding to the periods of high specific humidity. This may imply that the soil surface was wet, resulting in large evapotranspiration due to the wet soil and mature vegetation. Kondo *et al.* (1994) pointed out that a small diurnal range of Ts corresponds to a wet soil surface, while a large change is associated with a dry soil surface. This may not necessarily be the case when snow covers the soil surface above the soil thermometer. The diurnal range of Ts was very large, having values of 35°C to 45°C from mid-March to early June, which suggests that the soil surface was very dry and evapotranspiration very weak. In contrast, the diurnal range of Ts was small from mid-June to September, which may imply that the soil surface was wet and evapotranspiration very strong. There was about a one month lag between the disappearance of snow cover (as estimated by the abrupt decrease of albedo) and the sharp increase in both the air temperature, and Ts. During the period from late February to early March, the diurnal range of Ts was large, with values of about 20°C to 30°C. This range was larger than that during the period with continuous snow cover, but less than that in spring. From late February to early March, the daily minimum Ts was low — having values of -15°C to -25°C — while the daily maximum Ts was also low, exhibiting values

of 0°C to 10°C. One of the reasons why the daily mean air temperature and Ts were maintained at low values, despite the disappearance of snow cover from the surface, may be that any available energy to increase temperature was small since the large heat flux toward the ground was used for melting the frozen soil. This phenomenon should be related to the seasonal change in the large-scale circulation over the continent, although further study on this subject should be conducted.

### 3.2 Seasonal variations of the diurnal changes

As described in Subsection 3.1, abrupt changes in the air temperature and/or specific humidity were found at the transition points for each season by analyzing the AWS observed data at Baruunkharaa. Such phenomena might be related to both the exchange of air-masses and abrupt changes of the Bowen ratio, *i.e.*, the ratio of sensible heat flux to latent heat flux. Betts and Ball (1995) found that the diurnal curves of potential temperature  $\theta$  and specific humidity  $q$ , plotted on a  $(\theta, q)$  diagram, act as indirect estimates of the entrainment process of dry air from the lower free atmosphere to the boundary layer. It was also pointed out that with decreasing soil moisture (increase of the surface Bowen ratio), the diurnal range of air temperature increased, and

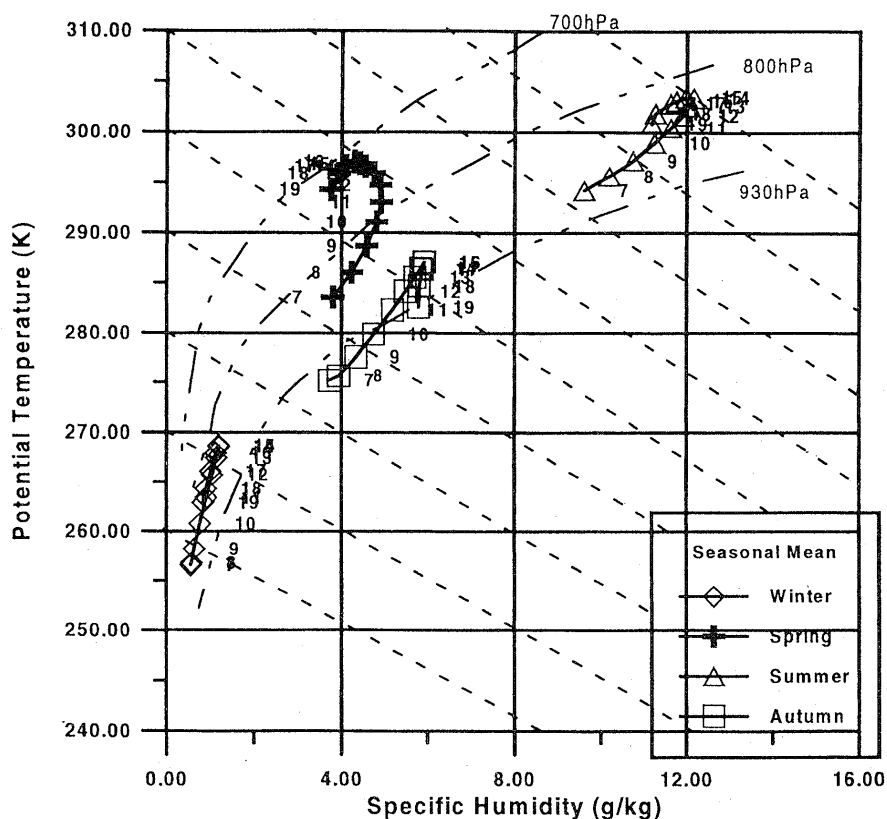


Fig. 6. Potential temperature  $\theta$  and specific humidity  $q$  on a  $(\theta, q)$  diagram for hourly data of seasonal mean values, *i.e.*, the four seasons as defined in 3.1, from 7:00 LST to 19:00 LST (GMT+8). The data are from October 1993 to September 1994 as observed at Baruunkharaa. The broken line indicates the isopleth of equivalent potential temperature. Dashed-and-double dotted line denotes isopleth of saturation pressure.

the afternoon decline of specific humidity increased on the  $(\theta, q)$  diagram, resulting in a rise of the lifting condensation level LCL. The diurnal range of both the equivalent potential temperature  $\theta_E$  and the difference between the saturation pressure, and the surface pressure  $P_{LCL}$ , can also be plotted on  $(\theta, q)$  diagram (Betts and Ball, 1995).

To clarify the seasonal march of near-surface atmospheric processes, diurnal cycles of  $\theta$  and  $q$ , which are related to the surface heat balance, are examined on the  $(\theta, q)$  diagram in terms of seasonal mean-hourly specific humidity values as shown in Fig. 6. In the discussion of the  $(\theta, q)$  plot, it is assumed that advection can be neglected and the site is located in a horizontally homogeneous grass land. Isopleths of both equivalent potential temperature ( $\theta_E$ ) and saturation pressure ( $p^*$ ) are also plotted. The seasonal means were calculated based on the four seasons defined in Subsection 3.1. Hourly values are plotted from 7:00 LST to 19:00 LST (GMT+8) for each season. The range of  $\theta$  increased by about 20K from the winter average to the spring average, and the daily maximum value of  $P_{LCL}$  increased from 100 hPa to 230 hPa. In the spring as  $\theta$  increased,

the specific humidity increased in the morning, but decreased in the afternoon (after 13:00 LST) as  $\theta$  continued to increase. It is likely that as the mixed layer expanded, drier air from the upper level was brought into the surface layer through entrainment, reducing the moisture content the surface layer. In the summer, although the diurnal range of  $\theta$  reaches its annual minimum of about 10K, and the diurnal range of specific humidity attained its annual maximum at a value of about  $3 \text{ gkg}^{-1}$ . During this season the daily maximum value of  $P_{LCL}$  decreases to its annual minimum at about 70 hPa. This suggests that evaporation from the surface was very large, and the cloud base low. During autumn the diurnal range of  $\theta$  was similar to that in exhibited spring, but the diurnal ranges of specific humidity and  $\theta_E$  were greater than those found in spring. Furthermore, there was no afternoon decrease in specific humidity, implying that the diurnal growth of the mixed layer was not sufficient to cause entrainment from above. The daily maximum value of  $P_{LCL}$  in autumn was less than that in spring, implying that the cloud base was lower than that found in spring. During both spring and autumn it is possible that



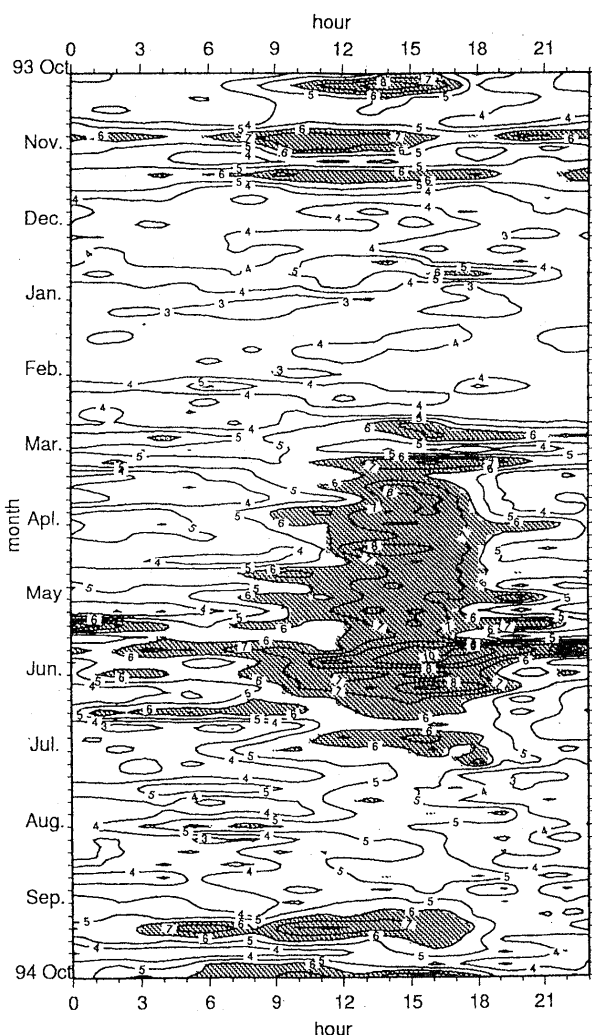


Fig. 7. Hour-month section of pentad mean values of maximum wind speed from October 1993 to September 1994 as observed at Baruunkharaa. Units are  $\text{ms}^{-1}$ . Contour interval is  $1 \text{ ms}^{-1}$ . Shaded area indicates maximum wind speeds excess of  $6 \text{ ms}^{-1}$ .

the surface stable layer is broken by growth of the daytime mixed layer, so that the diurnal range of air temperature becomes larger. No surface afternoon decrease of  $q$  is found in autumn, since the increase of  $q$  from the surface is greater than the decrease of  $q$  associated with the mixing of the free atmosphere as a result of the lower height of the daytime mixed layer.

The diurnal variation of wind speed is another measure of the diurnal growth of the mixed layer. Figure 7 shows a hour-month section of pentad mean values of maximum wind speeds from October 1993 to September 1994. The diurnal range of the winter maximum wind speed was small, having a value of about  $2 \text{ ms}^{-1}$  or less, suggesting the presence of a strong stable layer throughout the day (except from mid-February to early March). From mid-March to

early June, the diurnal range of the wind speed was large, exceeding about  $4 \text{ ms}^{-1}$  or more, while the wind speed reached its daily maximum from 13:00 LST to 15:00 LST, corresponding to the time of the afternoon decline of specific humidity that characterized the plot on the  $(\theta, q)$  diagram as shown in Fig. 6. As described in Subsection 3.1, the spring-time diurnal range of  $T_s$  was large due to strong solar radiation. These results strongly suggest that the growth of the mixed layer was sufficient enough to increase entrainment as a result of the strong spring heating from the surface. The diurnal range of the summertime maximum wind speed was small, being about  $2 \text{ ms}^{-1}$  or less. The diurnal range of the autumn maximum wind speed was about  $3 \text{ ms}^{-1}$  or less, and variable compared to spring. The reason for the daytime spring increase in the wind speed might be that the wind speed was suppressed by the surface stable layer in the morning, and then increased in the daytime as a result of the mixed layer entraining stronger winds from the upper layers.

#### 4. Concluding remarks

To investigate the role of land-atmosphere interactions in the formation and seasonal change of the surface climate over a continent, an analysis was conducted of continuously observed data. Seasonal and diurnal variations of the surface meteorological elements have been observed by use of an automatic weather station (AWS) at Baruunkharaa located in northern Mongolia, since September 30 1993.

Abrupt changes were found in the air temperature and specific humidity seasonal cycles during the period from October 1993 to September 1994. The year was climatologically divided into four seasons, based on the timing of these abrupt changes: winter (mid-November to early March), spring (mid-March to early June), summer (mid-June to late August), and autumn (early September to early November).

Air temperatures decreased by about  $20^\circ\text{C}$  concurrently with an increase in albedo of 0.5 to 0.9 during several days in mid-November. The winter air temperature remained at a constant level of  $-15^\circ\text{C}$  or less, exhibiting the characteristic of a coreless-type winter. The air temperature sharply increased by about  $20^\circ\text{C}$  to near the freezing point during several days in mid-March. The afternoon springtime decrease of specific humidity was dominant at around 13:00 LST. The diurnal range of maximum wind speed reached its annual maximum (about  $4 \text{ ms}^{-1}$  or more), corresponding to the time of the afternoon decrease in specific humidity. The springtime diurnal range of  $T_s$  was large, implying that the surface soil was very dry and evapotranspiration very weak. These results suggest that the diurnal growth of the mixed layer was sufficient to result in strong entrainment due to the strong springtime surface heating. During several days in

mid-June, an abrupt increase in specific humidity of about  $5 \text{ gkg}^{-1}$  occurred. The daytime increase of the specific humidity was more dominant than the other season on the  $(\theta, q)$  diagram, which likely indicates strong evaporation from the surface during the summer. The summertime diurnal range of  $T_s$  was small, suggesting a wet soil surface. The wet surface should be associated with strong evapotranspiration. Over several days in early September, the specific humidity decreased by about  $5 \text{ gkg}^{-1}$ . There was no afternoon decrease in specific humidity, implying that the development of the daytime mixed layer was not sufficient enough to result in strong entrainment from above. In autumn, the diurnal range of  $P_{LCL}$  was less than that found in spring. The characteristic air temperature of the coreless winter might be related to the stable conditions of the near surface layer found under the Siberian high, likely maintained by the strong radiative cooling that occurs over Mongolia and Siberia. The abrupt changes that occurred in specific humidity and the drastic change of the diurnal variation of  $\theta$  in the  $(\theta, q)$  diagram for mid-June may be related to the changes in the surface soil moisture and vegetation, which in turn may result in a great change in the Bowen ratio in determining the surface heat balance.

These phenomena strongly suggest that land surface-atmosphere interactions play important roles in the abrupt seasonal changes found in the seasonal cycle in the interior of the Eurasian Continent. Further analysis of the surface heat balance associated with continental-scale features of the seasonal change will be discussed in future studies.

#### Acknowledgments

The authors thank Mrs. Sosol Altanskh, the chief of the Baruunkharaa station, National Agency for Meteorology of Mongolia, for the maintenance of AWS. As part of GAME-AAN (the Asian AWS Network), this study was partly supported by the Asia-Pacific Network for Global Change Research and by the Special Research Fund for GAME from the Ministry of Education, Science, Sports and Culture (MESSC). This study was also supported by a Special Research Project on Global Environmental Change of the University of Tsukuba.

The first author would like to thank the staff members of the Environmental Research Center, University of Tsukuba, for much indirect support. Most of the figures are drawn using the GMT System (Wessel and Smith, 1991).

#### References

- Betts, A.K. and J.H. Ball, 1995: The FIFE surface diurnal cycle climate. *J. Geophys. Res.*, **100**, 25, 679-693.
- Ding, Y. and T.N. Krishnamurti, 1987: Heat Budget of the Siberian High and the Winter Monsoon. *Mon. Wea. Rev.*, **115**, 2428-2449.
- Groisman, P.Y., T.R. Karl and R.W. Knight, 1994: Changes of Snow Cover, Temperature, and Radiative Heat Balance over the Northern Hemisphere. *J. Climate*, **7**, 1633-1656.
- IPCC, 1992: *Climate Change 1992: The supplementary Report to the IPCC Scientific Assessment*. J.T. Houghton, B.A. Callander and S.K. Varney, (Eds.). Cambridge University Press, Cambridge, UK, 200pp.
- IPCC, 1995: *Climate Change 1995: The Science of Climate Change*. J.T. Houghton, L.G. Meira Filho, B.A. Callander, N. Harris, A. Kattenberg and K. Maskell (Eds.). Cambridge University Press, Cambridge, UK, 572pp.
- Kato, K., 1985: On the abrupt change in the structure of the Baiu front over China Continent in late May of 1979. *J. Meteor. Soc. Japan*, **63**, 20-36.
- Kato, K., 1987: Air mass transformation over the semi-arid region around North China and abrupt change in the structure of the Baiu front in early summer. *J. Meteor. Soc. Japan*, **65**, 737-750.
- Kato, K., J. Matsumoto and H. Iwasaki, 1995: Diurnal Variation of Cb-Clusters over China and Its Relation to Large-Scale Conditions in the Summer of 1979. *J. Meteor. Soc. Japan*, **73**, 1219-1234.
- Kondo, J.(Eds.) 1994: *Meteorology of the Water Environment — Water and Heat Balance of the Earth's Surface*, Asakura Shoten, 348pp (in Japanese).
- Van Loon, H., 1967: The Half-Yearly Oscillations in Middle and High Southern Latitudes and Coreless Winter. *J. Atmos. Sci.*, **24**, 472-486.
- Wessel, P. and W.H.F. Smith, 1991: Free software helps map and display data. *EOS Trans. AGU*, **72**, 441, 445-446.
- Yatagai, A. and T. Yasunari, 1994: Trends and Decadal-Scale Fluctuations of Surface Air Temperature and precipitation over China and Mongolia during the Recent 40 Year Period (1951-1990). *J. Meteor. Soc. Japan*, **72**, 937-957.

## AWS(自動気象観測装置)によって観測されたモンゴル北部の急激な季節変化

宮崎 真・安成哲三

(筑波大学地球科学系)

T. Adyasuren

(モンゴル国自然環境省)

モンゴル北部のバルンハラ (48°55'N, 106°4'E) において、自動気象観測装置 (AWS) によって、気候の季節変化における陸面過程の役割を明らかにするために、1993年の9月30日より地上気象要素の連続観測を行った。

1993年の10月から1994年の9月までのデータを解析したところ、気温または比湿の急激な変化(ジャンプ)により1年間を4つの季節に区分した。各季節の区分理由および特徴を以下に述べる。11月中旬に数日間で気温が約20°C低下したと同時に、アルベードは急激に0.5増加し、0.9になった(秋季→冬季)。冬季には、気温は-15°C以下のコアレス型(鍋底型)で、アルベードは2月中旬までは0.5以上と高く根雪があったと考えられる。3月中旬に気温が数日間で急激に約20°C上昇した(冬季→春季)。春季は、温位/比湿の日変化の特徴を表すダイアグラム(( $\theta, q$ )プロット)において、午後の比湿の減少が見られたこと、また地表面温度および風速の日較差が年間を通して最大であったこと、によって示唆される乾燥した地表面からの顕熱加熱による日中の混合層の発達により特徴づけられる。6月中旬に比湿が数日間で急激に5 gkg<sup>-1</sup>増加した(春季→夏季)。夏季には( $\theta, q$ )プロットにおいて、他の季節に比べると、温位の上昇に比べて比湿の増加がかなり大きく、地表面温度の日較差は小さかったことから、地表面からの蒸発が盛んであると推察される。9月上旬に比湿が数日間で5 gkg<sup>-1</sup>減少した(夏季→秋季)。秋季は( $\theta, q$ )プロットの傾きは、春季とほぼ同じであったが、午後の比湿の減少が見られなかったことから、エントレメントを引き起こすのに十分な日中の混合層の発達がなかったと推察される。